TECHNICAL ARTICLE

Optimization of Cutting Conditions, Parameters, and Cryogenic Heat Treatment for Surface Roughness in Milling of NiTi Shape Memory Alloy

Emre Altas, Omer Erkan, Dervis Ozkan, and Hasan Gokkaya

This study discusses the milling of Nickel-Titanium (NiTi) alloy, one of the innovative and widely used shape memory alloy (SMA). During the face milling operations, the average surface roughness (R_a) was investigated depending on the change in machining parameters, cutting conditions, and cryogenic heat treatment. Experiments were carried out with uncoated and two different coated (PVD, CVD) cutting tools with untreated, shallow ($-$ 80 °C) and deep ($-$ 196 °C) cryogenic heat treatment. In addition, experiments were carried out using Ethylene Glycol (EG), and boron added Ethylene Glycol (EG+5%BX) cutting fluids as well as dry cutting condition. In the cutting experiments, three different cutting speeds (20–35–50 m/min), three different feeds (0.03–0.07–0.14 mm/tooth), and 0.7 mm fixed cutting depth was used as machining parameters. In the milling mechanism of NiTi shape memory alloys, how the cutting parameters affect the surface quality is discussed in detail. In this context, the cutting parameters were successfully optimized using Taguchi and ANOVA methods. The study is innovative in terms of evaluating the effect of different cutting fluids and cryogenic heat treatment. The results showed that CVD-coated cutting tool, $-$ 196 °C cryogenic heat treatment, EG+5%BX cutting fluid, 50 m/min cutting speed, and 0.03 mm/tooth feed are the optimal parameters for the minor surface roughness. In addition, it has been determined that progress is the most influential parameter. On the other hand, ANOVA results showed that the most significant variable on the R_a was feed rate with 42.99%, and then cutting tool type 20.27%, cutting fluid 20.25%, cutting speed 11.68%, and cryogenic heat treatment 1.95%, respectively.

Keywords	ANOVA, cryogenic treatment, cutting fluids, NiTi SMA milling, taguchi optimization

Abbreviations	
ANOVA	Analysis of variance
a_p	Axial depth of cut (mm)
BUE	Built-Up Edge
None	Cryogenic process unapplied
CVD	Chemical vapor deposition
CI	Confidence interval
EG	Ethylene glycol
EG+%5BX	Boron added cutting fluid
f_z	Feed rate (mm/tooth)
MQL	Minimum quantity lubrication
NiTi	Nickel-Titanium
PVD	Physical vapor deposition
SEM	Scanning electron microscope
SMA	Shape memory alloy
SME	Shape Memory Effect
TiAlN	Titanium Aluminum Nitride
TiCN	Titanium Carbon Nitride
TiN	Titanium Nitride
R_a	Mean surface roughness (μm)
V_c	Cutting speed (m/min)

1. Introduction

Shape memory alloys (SMA) are materials that can gain their predefined shape or size when subjected to appropriate thermal and mechanical procedures. Studies on SMA materials are increasing day by day and their usage areas are expanding. This material group exhibits two different behaviors in itself: Shape Memory Effect (SME) and superelastisity (Ref 1). SMAs stand out with their mechanical properties such as corrosion resistance, SME and high strength. Compared to other SMAs, NiTi alloys have much better mechanical properties and SME makes this alloy valuable (Ref 2). On the contrary to these advantages, milling process of NiTi SMAs is quite problematic. Strain hardening, high ductility and low thermal conductivity of the alloy result in severe tool wear, poor surface finish, and

Emre Altas and **Dervis Ozkan**, Mechanical Engineering Department, Engineering Faculty, Bartın University, 74100 Bartin, Turkey; **Omer Erkan**, Mechanical Engineering Department, Faculty of Engineering, Düzce University, 81100 Duzce, Turkey; **Hasan Gokkaya**, Mechanical Engineering Department, Engineering Faculty, Karabuk University, 78050 Karabuk, Turkey. Contact e-mail: emrealtas@bartin.edu.tr.

poor machining efficiency, and it is difficult to meet dimensional accuracy requirements (Ref 3). In addition, the high ductility of the NiTi shape memory alloy is a source of the

hard-to-break chips that occur during machining. Therefore, the chip formation process of NiTi SMAs should be investigated (Ref 4, 5).

Many experiments and theoretical analysis have been performed to solve these problems (Ref 3). The use of coolants during the machining process is known to have positive effects on machinability. These positive results are mainly due to the effects of coolant on reducing the temperature, friction and wear amount at the tool-chip interface. It has been reported that cryogenic cooling has also positive effects on the machining of nickel-based superalloys (Ref 6) and titanium alloys (Ref 7). To increase cutting performance in machining of NiTi SMAs, coated cutting tools, the minimal amount of lubrication (MQL) and cryogenic cutting are used as green cutting technologies (Ref 4, 8).

In application of these solutions, the surface integrity is used in evaluation of the machinability of materials due to the fact that the performance of the products depends substantially on surface integrity of the material. General surface integrity properties used are average surface roughness (R_a), metallographic structure, residual stress, and work hardening. Velmurugan et al. reviewed the surface integrity properties of NiTi SMAs under the conventional, unconventional, and micromachining conditions (Ref 9). Kaynak et al. compared the R_a of the NiTi SMAs machined under two different conditions in the turning process with and without cryogenic coolant. As a result of the studies, the increase in the feed rate caused an increase in the R_a values. The R_a values obtained in the cryogenic machining condition were lower than those obtained in the dry machining condition in all feed parameters (Ref 10). Kulkarni et al., in their study of optimization of machining parameters in the processing of NiTi superelastic materials with wire erosion bench, investigated the effects of electrode advance, pulse duration, pulse interval time and the amount of voltage in the spark gap on the metal removal rate and R_a values. The researchers aimed to obtain the maximum metal removal rate and the minimum R_a value in line with the relevant parameters (Ref 1).

Weinert et al. investigated the best cutting conditions for machining NiTi SMAs and the effects of various cutting tool materials on the machinability of this material. Uncoated carbide, various PVD-coated carbides, CBN, PCD and ceramic tools were used as cutting tools. As a result of experimental studies, it has been shown that coated carbide cutting tools exhibit better machinability performance than uncoated carbide cutting tools (Ref 12). In a similar study, Guo et al. (Ref 13) investigated the surface integrity characteristics of $Ni_{50.8}Ti_{49.2}$ alloy after milling using AlTiN/TiN-coated carbide cutting tools (replaceable inserts using a single active insert). Huang investigated the effects of cutting parameters on tool wear and surface properties using high-speed milling. The authors reported that the increase in cutting speed resulted in an increase in the surface quality, and a decrease in the degree of work hardening. They attributed this to the decreasing of cutting forces due to reducing of chip thickness and chip cross-sectional area (Ref 14). Zhao et al. investigated the surface integrity of NiTi alloy during turning process with the change of cutting speed under cryogenic and dry conditions. They studied on microhardness, work contact layer, and phase transformation of the material. The authors reported that the machinability of the NiTi alloy depends highly on cutting speed (Ref 15). Kaynak et al. combined orthogonal experimentation, shear-induced phase transformation, and simulation and inves-

tigated the effect of phase transformation on surface integrity of the NiTi alloy (Ref 16). Zailani and Mativenga performed micro-milling experiments to compare the effects cooled air and MQL on the machinability of NiTi SMA. They reported that the cooled air can make the workpiece structure uniform, decrease the cutting force and the burr height. They also stated that chilled air and MQL have a big influence on decrease burr size, tool wear, and to increase surface roughness (Ref 17). Kaynak et al. studied on the machining induced deformation layer and investigated this layer's effect on the material's potential deformation behavior by experimental design methods. Researchers reported that cryogenic heat treatment causes a stronger effect than dry cutting (Ref 18). Aslantaş and Kaynak (Ref 19) investigated the effects of machining parameters on cutting forces, average surface roughness, and burr width in micro-milling and slot milling studies of $Ni_{55.82}Ti_{44.18}$ SMA. They stated that increasing cutting speed causes a phase transformation from austenite to martensite by increasing the stresses on the sample, and the hardening chips increase the cutting forces. Wang et al. (Ref 20) performed milling experiments to examine the effect of machining parameters on the strain hardening of $Ni_{50.8}Ti_{49.2}$ SMA. As a result of the experimental studies, they determined that the most important parameter affecting the strain hardening is the cutting speed. They stated that the austenite content of the machined surface is higher at high cutting speeds, and therefore, the strain hardening is higher. They found that an increase in the feed rate causes an increase in the shear force and plastic deformation area, and therefore an increase in strain hardening. Kuppuswamy and Yui (Ref 21) studied on the machining parameters in milling process of NiTi alloy to decrease cutting forces and burr formation. As a result of the experimental design, the researchers determined that the most important machining parameters to reduce the cutting forces and burr size in the micro-milling process of NiTi alloy are the cutting speed, feed rate, and depth of cut, respectively. Weinert and Petzoldt (Ref 22) investigated tool wear and machining quality in micro-milling processes of NiTi SMA using the MQL method. As a result of the experiments, they emphasized that the MQL method is necessary to achieve acceptable processing results. They found that the tool life increased, and the surface quality of the sample improved with the MQL method; high cutting width and feed rate provided better chip formation, increased tool life, and sample surface quality. Zhao et al. carried out experiments to examine the effect of cooling conditions on turning NiTi shape memory alloys at different cutting speeds. Tool wear, cutting force and surface morphology were determined as properties evaluated to investigate the effects of different cooling methods and stress-induced martensitic phase during the turning process. The study showed that the appearance of the stress-induced martensitic phase during the turning process impairs the machinability of NiTi shape memory alloys (Ref 23). Kabil et al. studied the optimization of the cutting parameters of NiTiHf high temperature shape memory alloys using a multi-objective optimization method. Empirical models were used to predict outputs in the turning process of NiTiHf and compared with experimental data. It has been determined that cutting parameters such as cutting speed, feed rate, and depth of cut have a great effect on performance. These parameters have been optimized using the Genetic Algorithm to achieve maximum tool life, minimum energy consumption, and maximum surface quality (Ref 24). Optimizing the R_a in milling is a method frequently used by

researchers. Many authors evaluated the R_a of different metal materials by optimizing with Taguchi method (Ref 25–30).

In the study, the effect of NiTi SMAs on R_a was investigated with the change of machining parameters under dry and MQL conditions with cutting fluids and tungsten carbide (WC) cutting tools with or without cryogenic heat treatment in face milling operations. Optimum cutting conditions and parameters were determined using the Taguchi method, an adequate experimental design method. Thus, recommendations have been made to ensure the surface integrity of this material, which is difficult to process.

2. Experimental Setup

Face milling was carried out to observe the influence of different machining parameters, cutting conditions, and cryogenic heat treatment parameters on the average surface roughness (R_a) of the NiTi SMA. Taguchi optimization was used to reduce the number of experiments. The milling tests were performed by three-axis "Falco VMC 855-B" industrial type CNC vertical machining center with 7.5 kW spindle power. R_a of the machined surface was measured by Mitutoyo Surftest SJ-310 tipped surface roughness measuring device because the R_a is the most commonly used parameter in roughness measurements in literature. After the surface roughness measurements of the milled samples were made, the data obtained were optimized and interpreted. The sampling length was chosen as $\lambda = 0.8$ mm and the evaluation length as $L = 5.6$ mm during the measurement. The schematic representation of the experimental setup is given in Fig. 1. Werte Mikro STN 25 operating at the pressure of 4-6 bar with a lubrication range of 0.0021-0.028 ml was used as the MQL system. The prepared cutting fluid was sprayed into the cutting medium with a nozzle on the system.

2.1 Material and Cutting Tools

NiTi SMA, used in orthopedics to join broken bones, was used as workpiece material in the experimental study. The NiTi SMA used was subjected to hot rolling after it was produced by the VAR (Vacuum Arc Remelting) method, and the material was in the austenite phase at room temperature. It contained 55.8% Ni element in its structure. NiTi SMA plate was prepared in $25 \times 100 \times 100$ mm dimensions. Detailed dimensions and plate photographs of the test sample are shown in Fig. 2. The chemical composition and mechanical properties of NiTi SMA are given in Tables 1 and 2, respectively (Ref 31).

Phase transformation temperatures of the alloy, i.e., martensite start (M_s), the martensite finish (M_f), austenite start (A_s), and austenite finish (A_f) temperature, were measured by DSC (Diffraction Scanning Calorimetry) method. According to the phase transformation temperatures given in Table 3, the NiTi alloy was seen to be in austenite phase at room temperature before machining.

Three different cutting tools belonging to Sandvik Coromant were utilized in the cutting experiments of NiTi SMAs in accordance with the test conditions specified in ISO 1832. These are uncoated, TiAlN coated (by PVD method), and TiN/Al_2O_3/TiCN coated (by CVD method with a TiN top layer) tungsten carbide cutting tools. To keep the cutting conditions constant during the experiments, each experiment was carried out using new cutting tools. In the experiments, a tool holder with a two-edge, 120 mm height (l_2), 25 mm cutting diameter (D_c), 17.06° tilt angle (λs) and the code R390-025A25-11L produced by Sandvik Coromant, suitable for replaceable inserts, was used. The geometry of the tool holder was
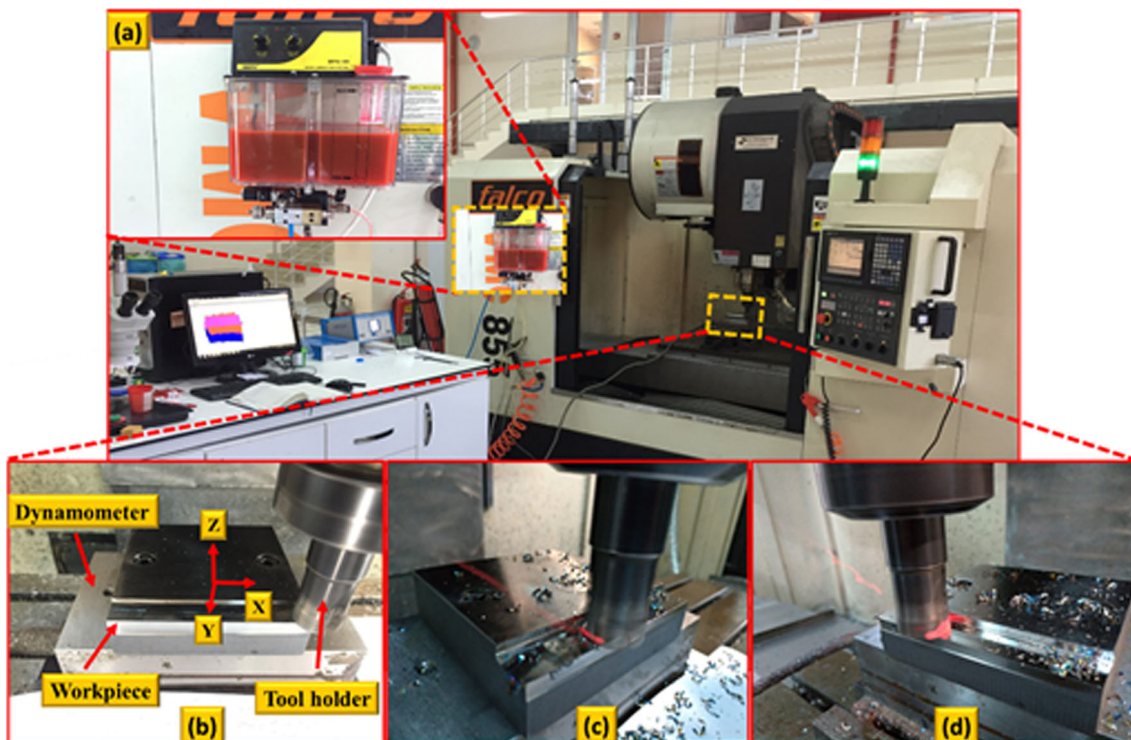

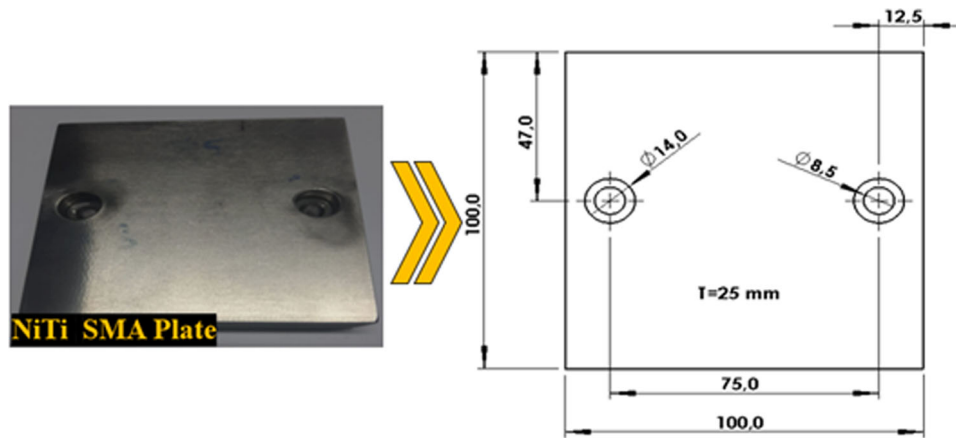**Fig. 1.** Experimental setup (a) MQL system, (b), (c) and (d) Milling of NiTi SMA plate

Fig. 2. NiTi plate and basic dimensions

Table 1. Chemical composition of NiTi SMA (%Weight) (Ref 31)

Ni	C	Co	Cu	Cr	H	Fe	Nb	N+O	Ti
55.8	0.038	0.005	0.006	0.004	0.001	0.0012	0.005	0.041	44.09

Table 2. Mechanical properties of NiTi SMA (Ref 31)

Yield stress, MPa	Tensile stress, MPa	Elongation %	Hardness (HRC)
280	630	13.9	26.5

Table 3. Phase transformation temperatures of the NiTi SMA (Ref 32)

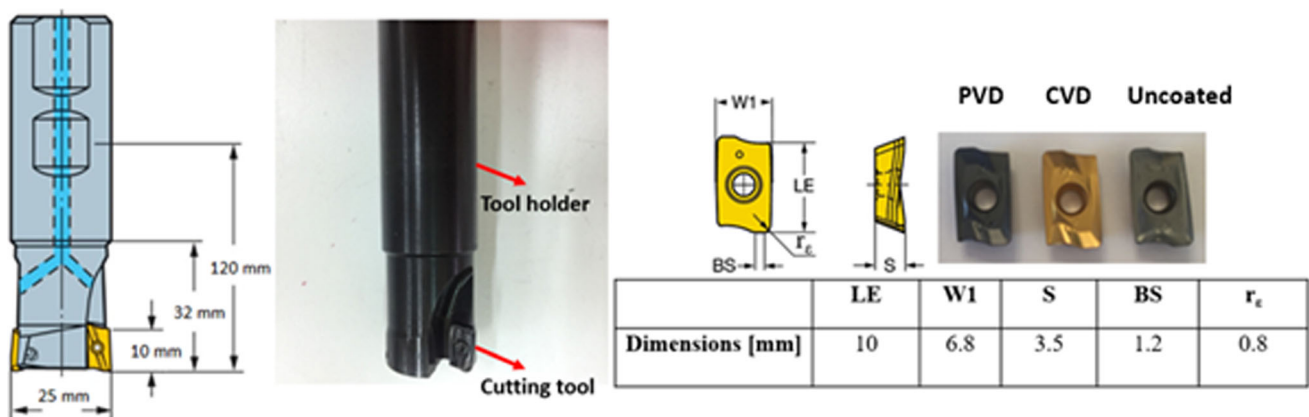| Melting method	Treatment	M_f, ºC	M_s, ºC	A_s, ºC	A_f, ºC
Vacuum arc method	Hot rolling	− 49.9	− 11.0	− 33.0	8.8

Fig. 3. Geometrical properties of the tool holder and cutting tools utilized in the cutting process

determined with reference to ISO 5608. Only one cutting tool was mounted onto the tool holder to provide a stable cutting conditions (Fig. 3).

2.2 Cutting Fluids and Cryogenic Process

Borax Decahydrate ($Na_2B_4O_7 \cdot 10H_2O$) and Ethylene Glycol (EG ($C_2H_6O_2$)) fluids were prepared as cutting fluid to be used

in milling operations of NiTi SMAs. These cutting fluids were applied onto the workpiece at an angle of 45° and from a distance of approximately 30 mm using the MQL (Minimum Quantity Lubrication) system. Borax Decahydrate is a natural alkaline mineral, and it consists of water, oxygen, sodium, and boron. As its alkaline (basic) structure, it acts as a reducing agent in the emulsion, allowing the pH level of the cutting fluid to be increased and the wear resistance to increase (Ref 33, 34). Borax Decahydrate (5% by weight BX) was added to Ethylene Glycol (EG), and boron added (EG+5%BX) cutting fluid was prepared. In order to obtain a homogeneous mixture, the formulated cutting fluids were mixed with a mechanical stirrer at 300 rpm at room temperature for 10 min and then placed in a magnetic stirrer (Ref 33, 35). The technical properties of the prepared cutting fluids are shown in Table 4.

Cryogenic heat treatment of cutting tools was carried out in a specially prepared computer-controlled cryogenic processing unit. Two different cryogenic heat treatments were applied to some carbide cutting tools at -80 ºC and -196 ºC, while the others were kept as untreated. In order to prevent microcracks that may occur in the cutting tools during cryogenic heat treatment, gradually cooling and heating process was applied to the cutting tools (Ref 36, 37). In order to relieve the stresses that may occur, the cutting tools were tempered by waiting at 200 °C for 2 h after the cryogenic heat treatment.

2.3 Experimental Parameters and Optimization

Uncoated, PVD-coated, and CVD-coated cutting tools were utilized in the cutting experiments of NiTi SMAs. Two different cryogenic heat treatment processes as shallow (-80 ºC) and deep (-196 ºC) were applied to some of cutting tools, while the others were kept untreated. Machining experiments were carried out in dry, EG, and EG+5%BX environments. Axial

depth of the cut ($a_p = 0.7$ mm) and radial cutting depths ($a_e = 15$ mm) were kept constant and three different cutting speeds (V_c) and feed rate (f_z) were determined as a result of preliminary experiments and suggestions of the cutting tool manufacturer as machining parameters. The processing parameters used are given in Table 5.

The Taguchi method was used to determine the optimum machining parameters and to analyze the effects of process parameters on the average surface roughness (R_a). The L_{27} orthogonal array was chosen as the experimental design. The experimental design created using the specified processing parameters is given in Table 6.

The effect of each machining parameter on the R_a was analyzed using the S/N ratio. In the Taguchi method, there are performance criteria as nominal best, smallest best, and largest best. The lowest value was taken for the best R_a value in the study, and the "smallest best" performance criterion was selected to calculate the lowest R_a value and the most

Table 4. Some physical properties of cutting fluids prepared for milling experiments (Ref 32)

Chemical	Property	Value
Boron added (EG+5%BX)	Density	1.73 g/cm³
	Melting point	741 °C
	Molecular weight	381.37 g/mol
	Heat capacity	4.0 J/g °C,
	pH	9.0-9.5
Ethylene glycol (EG)	Molecular weight	62.07 g/mol
	Density	1.13 g/cm³
	Viscosity	20.9 cp (20 °C)
	pH	6.0-8.0

Table 6. The experimental design L_{27}

Test No.	A	B	C	D	E
1	1	1	1	1	1
2	1	1	1	1	2
3	1	1	1	1	3
4	1	2	2	2	1
5	1	2	2	2	2
6	1	2	2	2	3
7	1	3	3	3	1
8	1	3	3	3	2
9	1	3	3	3	3
10	2	1	2	3	1
11	2	1	2	3	2
12	2	1	2	3	3
13	2	2	3	1	1
14	2	2	3	1	2
15	2	2	3	1	3
16	2	3	1	2	1
17	2	3	1	2	2
18	2	3	1	2	3
19	3	1	3	2	1
20	3	1	3	2	2
21	3	1	3	2	3
22	3	2	1	3	1
23	3	2	1	3	2
24	3	2	1	3	3
25	3	3	2	1	1
26	3	3	2	1	2
27	3	3	2	1	3

Table 5. Process parameters and their levels

		Level 1		
Code	Process parameters	1	2	3
A	Cutting tool	Uncoated	PVD	CVD
B	Cryogenic heat treatment	None	-80 ºC	-196 ºC
C	Cutting fluid	Dry	EG	EG+%5BX
D	Cutting speed, V_c (mm/min)	20	35	50
E	Feed rate, f_z (mm/tooth)	0.03	0.07	0.14

Table 7. R_a and Calculated S/N values relative to the L_{27} vertical index

| | **Machining parameters and their levels** | | | | | | |
| | **A** | **B** | **C** | **D** | **E** | | |
Experiment No.	**Cutting tool**	**Cryogenic heat treatment**	**Cutting fluid**	**Cutting speed V_c, m/min**	**Feed rate f_z (mm/tooth)**	**R_a, μm**	**Calculated S/N ratio (ni = 1-18), dB**
1	Uncoated	None	Dry	20	0.03	0.572	4.852
2	Uncoated	None	Dry	20	0.07	0.715	2,914
3	Uncoated	None	Dry	20	0.14	0.802	1.917
4	Uncoated	− 80 ºC	EG	35	0.03	0.520	5,680
5	Uncoated	− 80 ºC	EG	35	0.07	0.616	4.208
6	Uncoated	− 80 ºC	EG	35	0.14	0.728	2,757
7	Uncoated	− 196 ºC	EG+5%BX	50	0.03	0.380	8,404
8	Uncoated	− 196 ºC	EG+5%BX	50	0.07	0.472	6,521
9	Uncoated	− 196 ºC	EG+5%BX	50	0.14	0.540	5,352
10	PVD	None	EG	50	0.03	0.394	8,090
11	PVD	None	EG	50	0.07	0.452	6,897
12	PVD	None	EG	50	0.14	0.576	4,792
13	PVD	− 80 ºC	EG+5%BX	20	0.03	0.416	7,618
14	PVD	− 80 ºC	EG+5%BX	20	0.07	0.478	6,411
15	PVD	− 80 ºC	EG+5%BX	20	0.14	0.516	5,747
16	PVD	− 196 ºC	Dry	35	0.03	0.488	6,232
17	PVD	− 196 ºC	Dry	35	0.07	0.556	5,099
18	PVD	− 196 ºC	Dry	35	0.14	0.602	4.408
19	CVD	None	EG+5%BX	35	0.03	0.382	8,359
20	CVD	None	EG+5%BX	35	0.07	0.456	6,821
21	CVD	None	EG+5%BX	35	0.14	0.552	5,161
22	CVD	− 80 ºC	Dry	50	0.03	0.415	7,639
23	CVD	− 80 ºC	Dry	50	0.07	0.485	6,285
24	CVD	− 80 ºC	Dry	50	0.14	0.585	4,657
25	CVD	− 196 ºC	EG	20	0.03	0.424	7,453
26	CVD	− 196 ºC	EG	20	0.07	0.516	5,747
27	CVD	− 196 ºC	EG	20	0.14	0.602	4.408

appropriate S/N ratio for better product quality and the lowest cost. The "smallest best" performance characteristic is given in Eq **1**.

$$\frac{S}{N} = -10.\log\left(\frac{1}{n}\sum_{i=1}^{n} Y_i^2\right) \qquad \text{(Eq 1)}$$

In Eq **1**, Y is the average surface roughness, and n notates the number of experiments. The influence of the effect levels of the variables on the R_a was determined by applying ANOVA to the experimental results. Analysis of variance was performed with Minitab 18 software, taking into account the 95% confidence interval.

3. Results and Discussion

The sample R_a data obtained from the milling process of NiTi SMAs by the Taguchi L27 orthogonal test pattern and the S/N ratios calculated using Eq **1** are given in Table 7.

Figure 4 shows the relationship of the R_a with the machining parameters using average of S/N ratios and average of measured values.

According to the graphical display of S/N ratios Fig. 4(a), optimum test parameters for minimum R_a were defined as CVD cutting tool, − 196 °C cryogenic heat treatment, EG+5%BX cutting fluid, 50 m/min cutting speed, and 0.03 mm/tooth feed
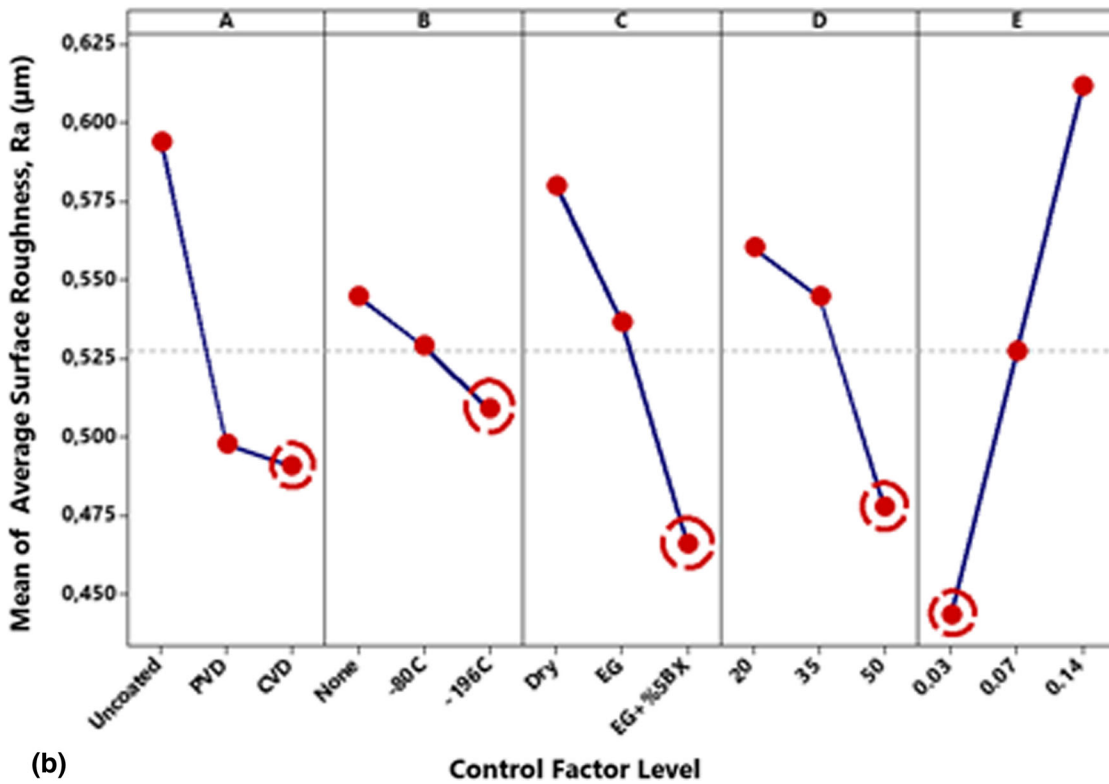
rate. In Fig. 5, the influence of machining parameters on the R_a is shown in 3D graphics.

When the influence of the coating materials on the R_a was examined, it was concluded that the coatings deposited to the cutting tools improved the R_a. The R_a value (0.490 μm) obtained using the CVD-coated cutting tool was approximately 17% lower than the uncoated cutting tool (0.593 μm). It has been seen that the R_a value of CVD-coated tools is also lower than that of PVD-coated tools. This improvement was attributed to the friction coefficient and thickness of the coating on the CVD-coated tools. These tools have a top TiN coating layer with a low friction coefficient which decreases chip sticking on the tool and makes chip formation easy. In addition, higher thickness of multilayer coating on these tools result in a larger cutting edge radius, which decreases the R_a in accordance with surface roughness theory. Accordingly, an improvement in the R_a of the sample was detected with CVD-coated cutting tools as seen in Ref. (Ref 38–41).

Applying cryogenic heat treatment to the cutting tools, a decrease was observed in the R_a values. The mean surface roughness value (0.508 μm) obtained using the deep cryogenic heat-treated cutting tool was approximately 7% lower than the value obtained in the non-cryogenic heat-treated cutting tool (0.544 μm). It is thought that the R_a decreases thanks to the preservation of the cutting edge geometry by delaying the tool wear as a result of the increase in the hardness and wear resistance of the cutting tools, especially with deep cryogenic heat treatment (Ref 36, 42). As for the influence of cutting
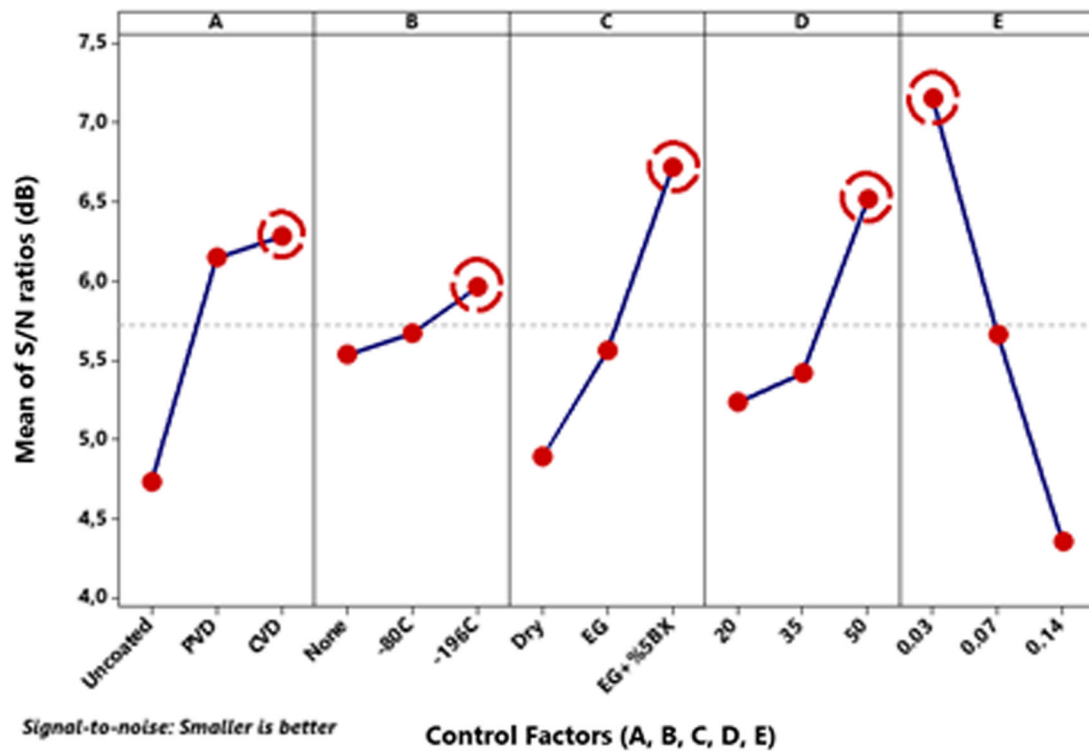
Fig. 4. Effect of machining parameters on the R_a of NiTi SMA in milling depending on (a) average of S/N ratios, (b) average of measured values

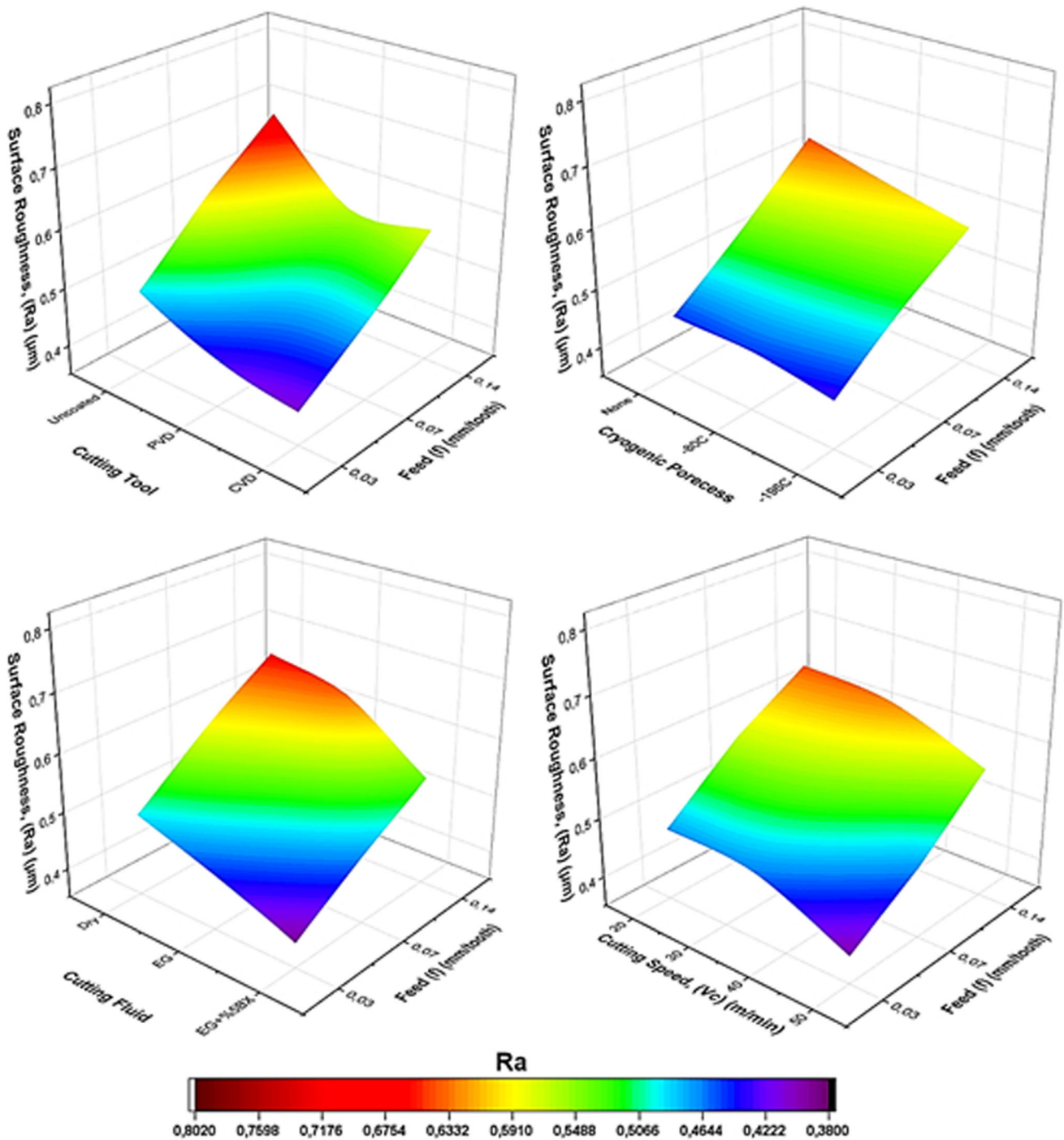**Fig. 5.** Influence of cutting parameters on the R_a

fluids on the R_a, a decrease was found in the R_a in the case of using EG and EG+5%BX cutting fluids. The R_a value (0.465 μm) obtained using EG+5%BX cutting fluid was approximately 20% lower than the value in dry cutting conditions (0.580 μm). In particular, high thermal conductivity and lubricating properties of EG+5%BX provided removal of the temperature in the cutting zone, reduction of the friction between the cutting tool and the sample, thereby reducing the temperature in the cutting zone. Depending on the decrease in friction and cutting temperature, tool hardness is preserved, preventing tool wear and the change of tool geometry. Thus, a

reduction of R_a has been observed as observed by Ref 33, 35. As for the effect of the cutting speed on the R_a, it was concluded that the R_a decreased with the increase in the cutting speed. It is thought that at low cutting speeds (20 m/min), the build-up edge (BUE) depositing on the cutting edge acts as a part of the cutting tool, which in turn increases the R_a by changing cutting tool geometry and thus the depth of cut Fig. 6(a) (Ref 43). The improvement of the R_a with the increase in cutting speeds can be explained by the fact that less strain hardening is obtained as the cutting temperature increases at high cutting speed and the chip formation around the cutting
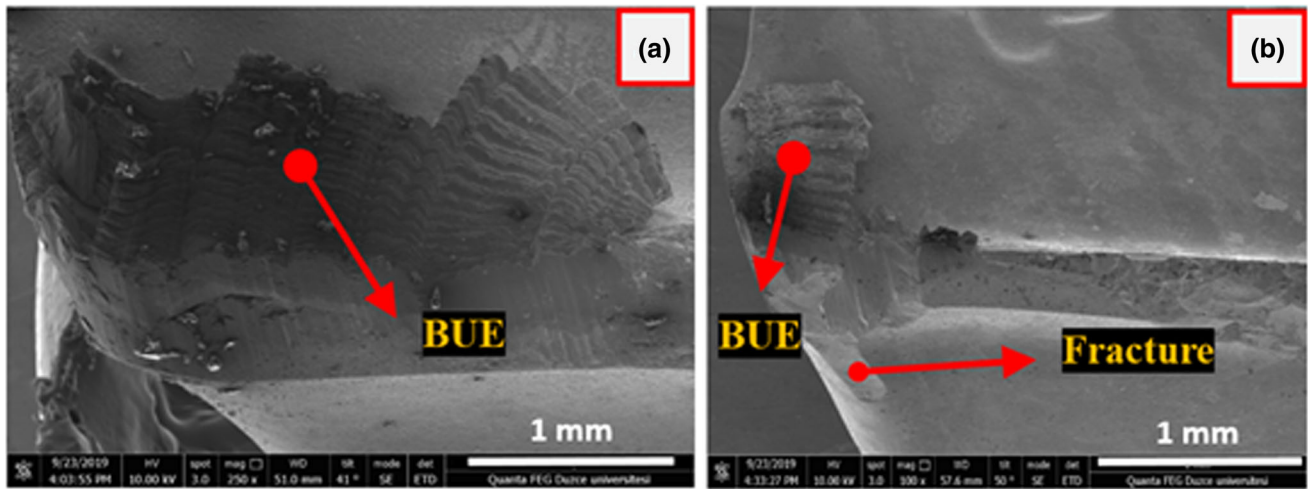
Fig. 6. (a) BUE formed on the cutting tool due to milling NiTi SMA in different machining parameters (0.03 mm/tooth feed rate) (b) SEM image of tool wear at high feed rate (0.14 mm/tooth)

edge is facilitated as explained by Ref 31. The R_a value (0.477 μm) obtained at high cutting speed (50 m/min) was approximately 15% lower compared to low cutting speed (20 m/min) value (0.560 μm). The improvement in the R_a due to the increase in cutting speed is an expected feature and the results are in good agreement with the literature (Ref 31, 44).

The wear on the cutting tool was visualized using a SEM microscope. Figure 6(a) shows the BUE formed, while Fig. 6(b) shows the high feed BUE and tooltip breakage.

As the feed rate increases, the cutting temperature increased due to the rise of chip width and the amount of removed chips. It is known that the generated heat is concentrated at the tool-chip and tool-workpiece interface due to the low thermal conductivity of NiTi SMA. It is an expected result that the R_a values will increase since the permanent stresses on the machined surface will increase with the feed rate similar to Ref 44, 45. The high R_a at a high feed rate (0.14 mm/tooth) is due to cutting tool wear Fig. 6(b). The cutting forces increase with the feed rate due to the increase in chip thickness. Accordingly, the wear formation on the tool accelerates and causes an increase in the R_a as seen in Ref. 31, 46. Finally, the increase in feed rate results in an increase in the R_a in accordance with the surface roughness theory.

So as to show the influence of optimum cutting parameters on the R_a, the experiments at three different machining parameters were carried out. The surface roughness profiles obtained at these machining conditions are shown in Fig. 7. The profiles show that the lowest R_a (0.324 μm) was obtained at optimum cutting parameters (CVD cutting tool, $-$ 196 °C cryogenic heat treatment, EG+5%BX cutting fluid, 50 m/min cutting speed, and 0.03 mm/tooth feed rate. The height of the roughness peaks decreased and the peaks became frequent.

In order to determine the effects of each machining parameter on the R_a in milling of NiTi SMA, ANOVA analysis was performed. It was seen that ANOVA analysis was carried out at a 95% confidence level. The parameters and levels that affect the R_a values are given in Table 8.

According to ANOVA results, it was determined that the variable that have the most significant effect on the R_a is the feed rate with 42.99% contribution. It was followed by the cutting tool type by 20.27%, the cutting fluid by 20.25%, the cutting speed by 11.68%, and the cryogenic heat treatment by

1.95%. The main effect plot shown in Fig. 4 and the S/N response values indicated in Table 8 confirmed the analysis of variance. The error in the ANOVA table remained at the level of 2.87%. Since the error effect rates in the ANOVA table are expected to be below 20% for a safe result (Ref 47), it can be stated that the ANOVA results met the standards in this study. According to the regression analysis results, the correlation coefficients established for the R_a are R^2 = 97.13%, R^2_{adj} = 95.34%, and R^2_{pred} = 91.83%. These results show that the model obtained for the mean surface roughness agrees with the experimental data and has a high predictive ability.

The normal probability plot of the residuals and histogram of residuals were used to verify normality assumption. As seen from Fig. 8(a,c), the residuals fall approximately along a straight line, and this means that the errors are in the normal distribution and the terms mentioned in the model are the only significant (Ref 48, 49). There is no systematic pattern and unusual structure Fig. 8(b, d). This means that the model obtained is adequate and there is no doubt for any violation of independence or constant variance assumption (Ref 50, 51).

3.1 Confirmation Experiments and Calculation of Confidence Interval for Average Surface Roughness

After the optimum experiment parameters were determined, the reliability of the optimized parameters is experimentally validated in order to obtain reliable experimental results at a 95% confidence interval and 5% significance level. Three validation experiments were performed in milling operations, and the arithmetic average of the results is given in Table 9. Optimal (CVD-coated cutting tool, $-$ 196 °C cryogenic heat treatment, EG+5%BX coolant, 50 m/min cutting speed and 0.03 mm/tooth feed rate) and predicted (CVD-coated cutting tool, $-$ 196 °C cryogenic heat treatment, EG+5%BX coolant, 50 m/min cutting speed and 0.03 mm/tooth feed rate) machining parameter combinations for minimum R_a were compared in Table 9. According to these comparisons, the estimated R_a value was 0.357 μm, while the R_a value experimentally obtained was 0.324 μm.

In order to determine the reliability of the optimization process with the Taguchi method, the confidence interval of the estimated values should be determined. For this purpose, Eq 2
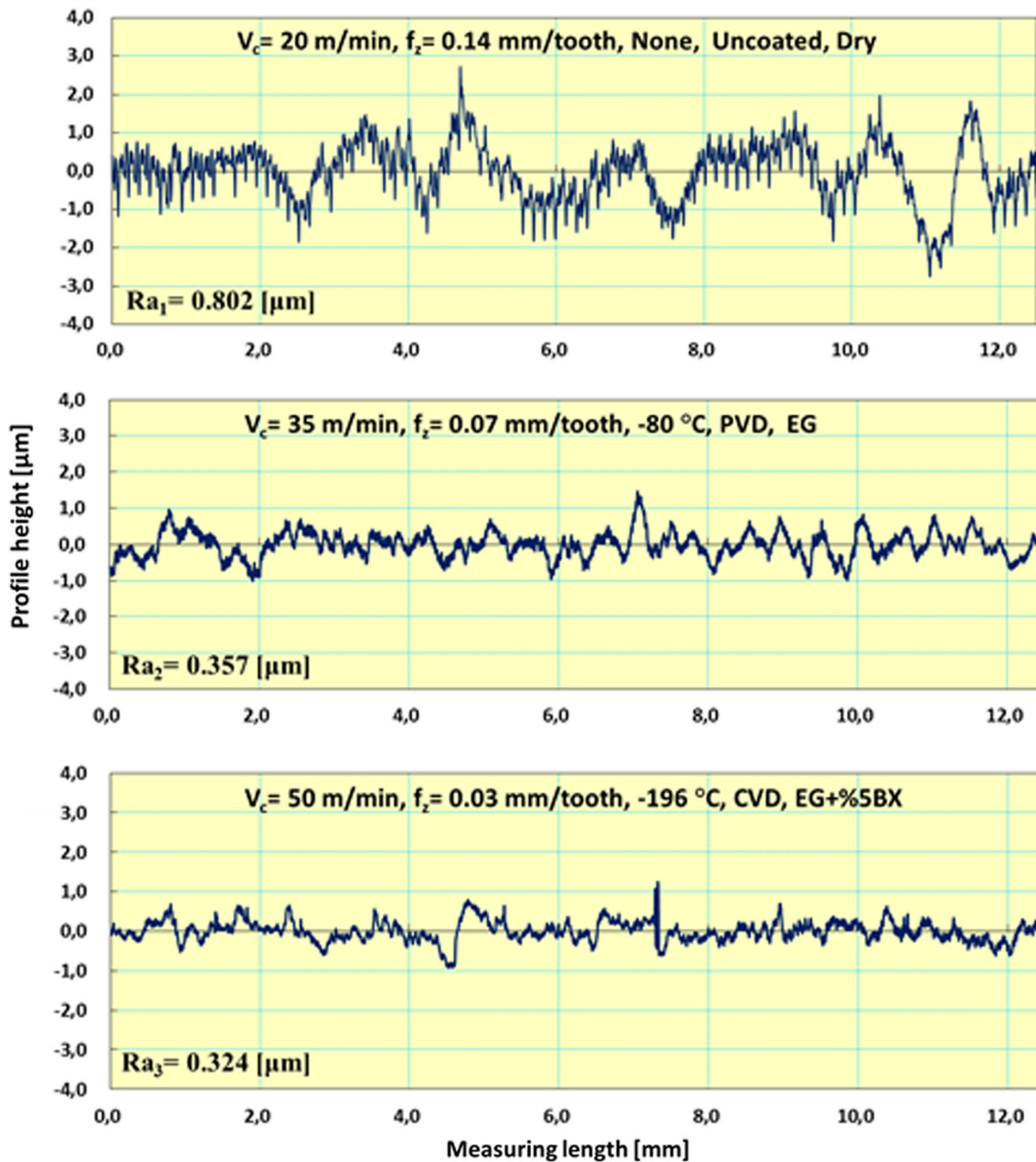
Fig. 7. Surface roughness profiles of NiTi SMA after milling at different cutting parameters

Table 8. ANOVA results for the R_a value obtained with different machining parameters in the milling process of NiTi SMA

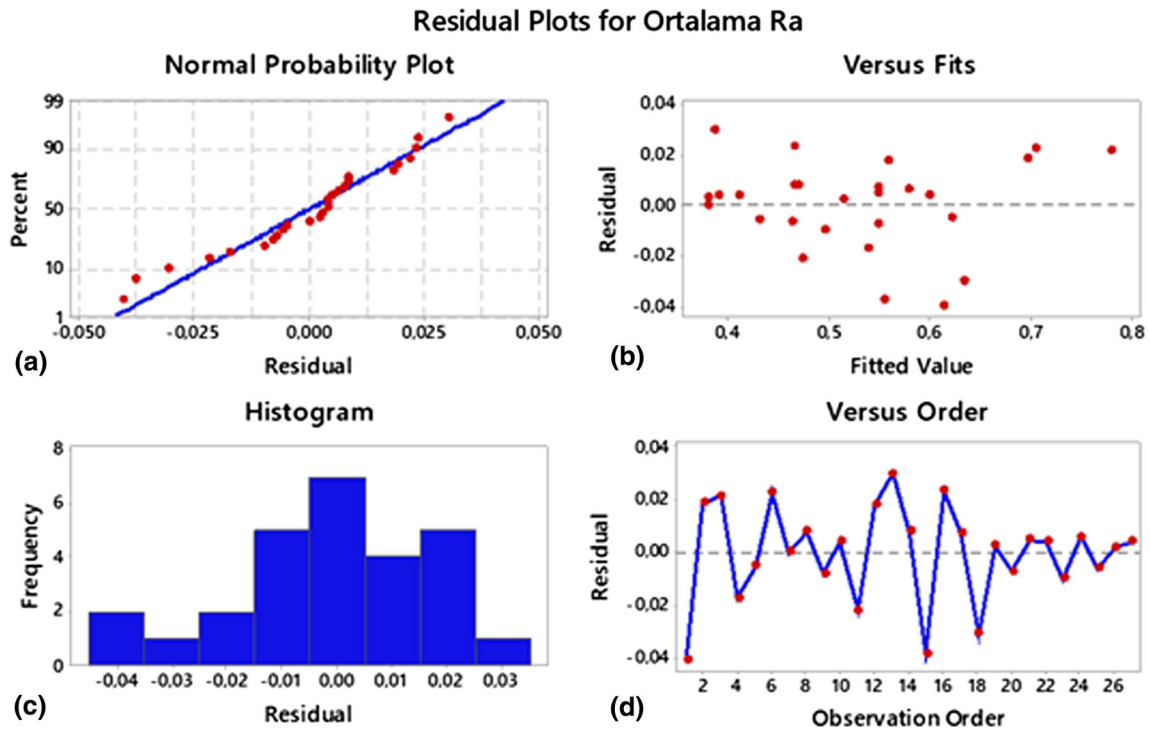| Variance source	Degree of freedom (df)	Sum of squares (SS)	Mean square (MS)	F	P	Contribution, %
A	2	0.059874	0.029937	56.51	0.001	20.27
B	2	0.00575	0.002875	5.43	0.016	1.95
C	2	0.059813	0.029906	56.45	0.001	20.25
D	2	0.034505	0.017253	32.57	0.001	11.68
E	2	0.127008	0.063504	119.87	0.001	**42.99**
Error	16	0.008477	0.00053			2.87
Total	26	0.295427				100.00
S = 0.0230171 R^2 = 97.13% $R^2_{(adj)}$ = 95.34%						

Fig. 8. (a) Normal probability plot for standardized residuals (b) versus fits for standardize residuals (c) histogram of standardized residuals (d) versus order for standardize residuals

Table 9. Comparison of the measured and estimated values according to Taguchi design for the R_a value obtained from the milling process of NiTi SMA at different machining parameters

Taguchi optimization	Initial machining parameters	Optimum machining parameters	
		Estimated	Experimental
Cutting conditions	PVD, − 80 °C EG+5%BX, 35, 0.07	CVD, − 196 °C, EG+5%BX, 50, 0.03	CVD, − 196 °C, EG+5%BX, 50, 0.03
Average surface roughness R_a (μm)	0.386	0.357	0.324
S/N ratio (dB)	8,971	9,734	10,933

Table 10. Confidence interval (CI) formulas and symbols (Ref 31)

NS.	Symbol	Explanation
1	$F_{\alpha;1;V_2}$	F ratio 95% (according to F chart)
2	α	severity level
3	V_2	degrees of freedom error
4	V_e	Error variance
5	r	Number of repetitions for validation
6	n_{eff}	The effective number of repetitions
7	T_{exp}	Total number of experiments
8	T_{dof}	Total principal factor degrees of freedom

Fig. 9. Comparison of predicted and experimental values for output parameters

was used to obtain the confidence interval (CI) for the estimated average surface roughness (R_{a_opt}). CI symbols and abbreviations of Eq 2 and 3 are given in Table 10.
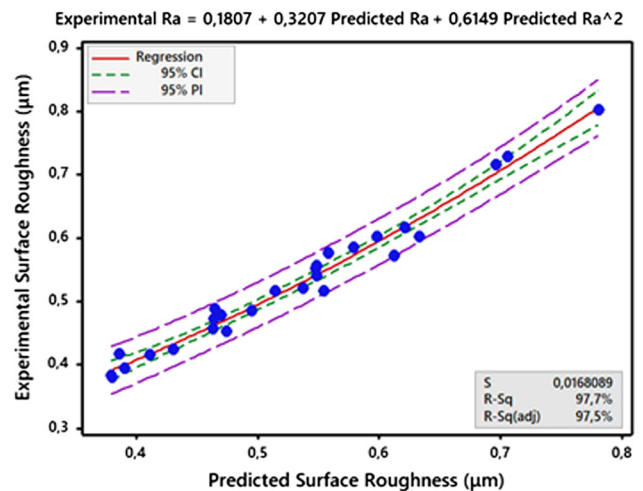
$$CI = \sqrt{F_{\alpha:1,V2} \cdot V_e \cdot \left(\frac{1}{n_{\text{eff}}} + \frac{1}{r}\right)} \qquad \text{(Eq 2)}$$

$$n_{\text{eff}} = \frac{T_{\text{exp}}}{1 + T_{\text{dof}}} \qquad \text{(Eq 3)}$$

The optimum average surface roughness ($R_{a\_opt} = 0.357$ μm) estimated by the optimization process is given in Table 9. In the calculation in Eq (2), $\alpha = 0.05$, $F_{\alpha:1,V1} = 4.747$ (95% F ratio (F table)), and $R_a = 0.00053$ (Table 8), $r = 3$, $T_{\text{exp}} = 27$, $T_{\text{dof}} = 10$ and $n_{\text{eff}} = 2.45$. Using Eq 2 and 3, the R_a was calculated as $CI_{Ra} = \pm 0.043$.

CI range for estimated average optimum surface roughness at 95% confidence interval and 5% significance level:

$$[R_{a\_opt} - CI_{Ra}] < Ra_{exp} < [R_{a\_opt} + CI_{Ra}]$$
$$\rightarrow [0.357 - 0.043] < 0.324 < [0.357 + 0.043]$$
$$= 0.314 < 0.324 < 0.400.$$

Due to the fact that the average surface roughness value ($R_{aexp} = 0.324$ μm) obtained as a consequence of the validation experiments is in confidence interval, it was seen that the optimization is successful by Taguchi method at a significance level of 0.05.

Figure 9 shows the comparison of predicted and experimental values for the R_a. It is seen that all experiment results fall in the confidence interval (CI) and prediction interval (PI). This means that the model can be used in estimation of the R_a.

4. Conclusions

In the study, the influence of cutting conditions and machining parameters on the R_a of NiTi SMA plates was investigated during face milling operations. The results clearly revealed that feed rate, cutting fluid and deep cryogenic heat treatment are highly effective on R_a. The other experimental and optimization results are listed as follows:

- According to Taguchi optimization, the most significant parameter on the R_a is the feed rate; it is followed by cutting tool, cutting fluid, cutting speed and cryogenic heat treatment, respectively.
- The R_a increases with the feed rate, while it decreases with the cutting speed, at especially high values of the cutting speed by about 15%.
- The R_a value obtained by CVD-coated tools is lower than that of PVD-coated tools; it is approximately 16% lower compared to the uncoated tool.
- Deep cryogenic heat-treated tools provides an approximately 7% lower mean surface roughness.
- Usage of the EG and EG+5%BX cutting fluids leads to a 20% decrease in the R_a compared to the dry machining condition.
- The optimum test parameters for the R_a are the S40T grade cutting tool, $-$ 196 °C cryogenic heat treatment, EG+5%BX cutting fluid, 50 m/min cutting speed, and 0.03 mm/tooth feed.
- BUE and breakage on the cutting tool occurring especially at high feed rate are responsible for the increase in average surface roughness.

References

1. E. Farber, J.-N. Zhu, A. Popovich and V. Popovich, A Review of NiTi Shape Memory Alloy as a Smart Material Produced by Additive Manufacturing, *Mater. Today Proc.*, 2020, **30**(3), p 761–767
2. S. Bahl, H. Nagar, I. Singh and S. Sehgal, Smart Materials Types, Properties and Applications: A Review, *Mater. Today Proc.*, 2020, **28**(3), p 1302–1306
3. B. Dash, M. Das, M. Das, T.R. Mahapatra and D. Mishra, A Concise Review on Machinability of NiTi Shape Memory Alloys, *Mater. Today Proc.*, 2019, **18**, p 5141–5150
4. F. Pusavec, H. Hamdi, J. Kopac and I. Jawahir, Surface Integrity in Cryogenic Machining of Nickel Based Alloy—Inconel 718, *J. Mater. Process. Technol.*, 2011, **211**(4), p 773–783
5. M. Bermingham, J. Kirsch, S. Sun, S. Palanisamy and M. Dargusch, New Observations on Tool Life, Cutting Forces and Chip Morphology in Cryogenic Machining Ti-6Al-4V, *Int. J. Mach. Tools Manuf*, 2011, **51**(6), p 500–511
6. Y. Zhao, J. Li, K. Guo, V. Sivalingam and J. Sun, Study on chip formation characteristics in turning NiTi shape memory alloys, *J. Manuf. Process.*, 2020, **58**, p 787–795
7. R. Ashima, A. Haleem, S. Bahl, M. Javaid, S.K. Mahla and S. Singh, Automation and Manufacturing of Smart Materials in Additive Manufacturing Technologies Using Internet of Things Towards the Adoption of Industry 4.0, *Mater. Today Proc.*, 2021, **45**(6), p 5081–5088
8. G. Wang, Z. Liu, J. Niu, W. Huang and Q. Xu, Work Hardening Influencing on Shape Memory Effect of NiTi Alloy by Varying Milling Speeds, *Smart Mater. Struct.*, 2019, **28**(10), p 105034
9. C. Velmurugan, V. Senthilkumar, S. Dinesh and D. Arulkirubakaran, Machining of NiTi-Shape Memory Alloys: A Review, *Mach. Sci. Technol.*, 2018, **22**(3), p 355–401
10. Y. Kaynak, H. Karaca, I.S. Jawahir, Cryogenic Machining of NiTi Shape Memory Alloys, 6th International Conference and Exhibition on Design and Production of MACHINES and DIES/MOLDS, 2011
11. V.N. Kulkarni, V. Gaitonde, V. Hadimani, V. Aiholi, Optimization in Wire Electric Discharge Machining of Nickel-Titanium Shape Memory Alloy, IOP Conference Series: Materials Science and Engineering, IOP Publishing., 2019, **577**, p 012015
12. K. Weinert, V. Petzoldt and D. Kötter, Turning and Drilling of NiTi Shape Memory Alloys, *CIRP Ann.*, 2004, **53**(1), p 65–68
13. Y. Guo, A. Klink, C. Fu and J. Snyder, Machinability and Surface Integrity of Nitinol Shape Memory Alloy, *CIRP Ann.*, 2013, **62**(1), p 83–86
14. H. Huang, A Study of High-Speed Milling Characteristics of Nitinol, *Mater. Manuf. Process.*, 2004, **19**(2), p 159–175
15. Y.-Z. Zhao, K. Guo, V. Sivalingam, J.-F. Li, Q.-D. Sun, Z.-J. Zhu, J. Sun, Surface Integrity Evolution of Machined NiTi Shape Memory Alloys After Turning Process, *Adv. Manufact.* 2021, **9**(3), p 446–456
16. Y. Kaynak, H.E. Karaca and I.S. Jawahir, Cutting Speed Dependent Microstructure and Transformation Behavior of NiTi Alloy in Dry and Cryogenic Machining, *J. Mater. Eng. Perform.*, 2015, **24**(1), p 452–460
17. Z.A. Zailani and P.T. Mativenga, Effects of Chilled Air on Machinability of NiTi Shape Memory Alloy, *Proc. CIRP.*, 2016, **45**(Supplement C), p 207–210
18. Y. Kaynak, H. Tobe, R.D. Noebe, H.E. Karaca and I.S. Jawahir, The Effects of Machining on the Microstructure and Transformation Behavior of NiTi Alloy, *Scripta Mater.*, 2014, **74**(Supplement C), p 60–63
19. K. Aslantaş and Y. Kaynak, Micro Milling of NiTi Shape Memory Alloy and Determination of Critical Chip Thickness, *J. Faculty Eng. Architect. Gazi Univ.*, 2018, **2018**(18–2), p 2–16

20. G. Wang, Z. Liu, X. Ai, W. Huang and J. Niu, Effect of Cutting Parameters on Strain Hardening of Nickel-Titanium Shape Memory Alloy, *Smart Mater. Struct.*, 2018, **27**(7), p 075027

21. R. Kuppuswamy and A. Yui, High-Speed Micromachining Characteristics for the NiTi Shape Memory Alloys, *Int. J. Adv. Manufact. Technol.*, 2017, **93**(1), p 11–21

22. K. Weinert and V. Petzoldt, Machining NiTi Micro-Parts by Micro-Milling, *Mater. Sci. Eng.A.*, 2008, **481–482**(12), p 672–675

23. Y. Zhao, K. Guo, J. Li and J. Sun, Investigation on Machinability of NiTi Shape Memory Alloys Under Different Cooling Conditions, *Int. J. Adv. Manufact. Technol.*, 2021, **116**(5), p 1913–1923

24. A. Kabil, Y. Kaynak, H. Saruhan and O. Benafan, Multi-objective Optimization of Cutting Parameters for Machining Process of Ni-Rich NiTiHf High-Temperature Shape Memory Alloy Using Genetic Algorithm, *Shape Memory Superelast.*, 2021, **7**(2), p 270–279

25. E. Nas, G. Samtaş and H. Demir, Mathematically Modeling Parameters Influencing Surface Roughness in CNC Milling, *Pamukkale Univ. J. Eng. Sci.*, 2012, **18**(1), p 47–59

26. M. Ayyildiz, Modeling for Prediction of Surface Roughness In Milling Medium Density Fiberboard with a Parallel Robot, *Sens. Rev.*, 2019, **39**(5), p 716–723

27. F. Kura, Optimization of Cutting Parameters in Finishing Milling of Hardox 400 Steel, *Int. J. Anal. Exp. Finite Elem. Anal.*, 2018, **5**(3), p 44–49

28. M.O.J.Z.B. PLASTIKE, Optimization of Surface Roughness in Finish Milling of AISI P20+ S Plastic-Mold Steel, *Optimization* 2018, **52**(2): 195-200

29. K. Aslantas, E. Ekici and A. Cicek, Optimization of Process Parameters for Micro Milling of Ti-6Al-4V Alloy Using Taguchi-Based Gray Relational Analysis, *Measurement*, 2018, **128**, p 419–427

30. Y. Harun, H. Demir and G. Arif, Optimization of the Cutting Parameters Affecting the Surface Roughness on Free Form Surfaces, *Sigma J. Eng. Natl. Sci.*, 2017, **35**(2), p 323–331

31. E. Altas, H. Gokkaya, M.A. Karatas and D. Ozkan, Analysis of Surface Roughness and Flank Wear Using the Taguchi Method in Milling of NiTi Shape Memory Alloy with Uncoated Tools, *Coatings*, 2020, **10**(12), p 1259

32. E. Altas, M. Altin-Karatas, H. Gokkaya and Y. Akinay, Surface Integrity of NiTi Shape Memory Alloy in Milling with Cryogenic Heat Treated Cutting Tools under Different Cutting Conditions, *J. Mater. Eng. Perform.*, 2021, **30**, p 9426–9439

33. B. Kursuncu and A. Yaras, Assessment of the Effect of Borax and Boric Acid Additives in Cutting Fluids on Milling of AISI O2 Using MQL sysTem, *Int. J. Adv. Manufac. Technol.*, 2018, **95**(5), p 2005–2013

34. K. Kiliçay and M. Ulutan, Investigation of the Solid Lubrication Effect of Commercial Boron-Based Compounds in End Milling, *Int. J. Precis. Eng. Manuf.*, 2016, **17**(4), p 517–524

35. M.H. Cetin and S.K. Kilincarslan, Effects of Cutting Fluids with Nano-Silver and Borax Additives on Milling Performance of Aluminium Alloys, *J. Manuf. Process.*, 2020, **50**, p 170–182

36. S. Akincioğlu, H. Gökkaya and İ Uygur, A Review of Cryogenic Treatment on Cutting Tools, *Int. J. Adv. Manufact. Technol.*, 2015, **78**(9–12), p 1609–1627

37. A. Saini, B. Pabla and S. Dhami, Improvement in PERFORMANCE of Cryogenically Treated Tungsten Carbide Tools in Face Milling of Ti-6Al-4V Alloy, *Mater. Manuf. Process.*, 2020, **35**(5), p 598–607

38. H. Caliskan, P. Panjan, C. Kurbanoglu, Hard coatings on cutting tools and surface finish, 2017

39. W.F. Sales, J. Schoop, L.R. da Silva, Á.R. Machado and I. Jawahir, A Review of Surface Integrity in Machining of Hardened Steels, *J. Manuf. Process.*, 2020, **58**, p 136–162

40. M.A. Makhesana and K.M. Patel, Performance of PVD and CVD Coated Cutting Tool Inserts in Machining Under MQL-MQSL Environment, *Int. J. Mechatron. Manufact. Syst.*, 2020, **13**(3), p 210–229

41. F.J.G. Silva, R.P. Martinho, C. Martins, H. Lopes and R.M. Gouveia, Machining GX2CrNiMoN26-7-4 DSS Alloy Wear Analysis of TiAlN and TiCN/Al2O3/TiN Coated Carbide Tools Behavior in Rough End Milling Operations, *Coatings*, 2019, **9**(6), p 392

42. A. Palanisamy, T. Selvaraj and S. Sivasankaran, Optimization of Turning Parameters of Machining Incoloy 800H Superalloy Using Cryogenically Treated Multilayer CVD-Coated Tool, *Arab. J. Sci. Eng.*, 2018, **43**(9), p 4977–4990

43. H. Gökkaya, The Effects of Machining Parameters on Cutting Forces, Surface Roughness, Built-Up Edge (BUE) and Built-Up Layer (BUL) During Machining AA2014 (T4) Alloy, *Strojniski Vestnik J. Mech. Eng.* 2010, **56**(9), p 584–593

44. Y. Kaynak, B. Huang, H.E. Karaca and I.S. Jawahir, Surface Characteristics of Machined NiTi Shape Memory Alloy: The Effects of Cryogenic Cooling and Preheating Conditions, *J. Mater. Eng. Perform.*, 2017, **26**(7), p 3597–3606

45. Y. Kaynak, H.E. Karaca, R.D. Noebe and I.S. Jawahir, Tool-Wear Analysis in Cryogenic Machining of NiTi Shape Memory Alloys: A Comparison of Tool-Wear Performance with Dry and MQL Machining, *Wear*, 2013, **306**(1), p 51–63

46. E. Kaya, İ. Kaya, Tool Wear Progression of PCD and PCBN Cutting Tools in High Speed Machining of NiTi Shape Memory Alloy Under Various Cutting Speeds, *Diamond Related Mater.* 2020, p 1-10

47. V. Nguyen, T. Nguyen and D. Tien, Cutting Parameter Optimization in Finishing Milling of Ti-6Al-4V Titanium Alloy Under MQL Condition Using TOPSIS and ANOVA Analysis, *Eng. Technol. Appl. Sci. Res.*, 2021, **11**(1), p 6775–6780

48. E. Hazir and T. Ozcan, Response Surface Methodology Integrated with Desirability Function and Genetic Algorithm Approach for the Optimization of CNC Machining Parameters, *Arab. J. Sci. Eng.*, 2019, **44**(3), p 2795–2809

49. E. Hazir, E.S. Erdinler and K.H. Koc, Optimization of CNC Cutting Parameters Using Design of Experiment (DOE) and Desirability Function, *J. For. Res.*, 2018, **29**(5), p 1423–1434

50. M. Bahrami, M.J. Amiri, M.R. Mahmoudi and S. Koochaki, Modeling Caffeine Adsorption by Multi-Walled Carbon Nanotubes Using Multiple Polynomial Regression with Interaction Effects, *J. Water Health*, 2017, **15**(4), p 526–535

51. G. Mansour, P. Kyratsis, A. Korlos and D. Tzetzis, Investigation into the Effect of Cutting Conditions in Turning on the Surface Properties of Filament Winding GFRP Pipe Rings, *Machines.*, 2021, **9**(1), p 16